

2007

## Specific heat and magnetic relaxation analysis of MgB<sub>2</sub> bulk samples with and without additives

C. Senatore  
*University of Geneva*

P. Lezza  
*University of Geneva*

R. Lortz  
*University of Geneva*

Olga V. Shcherbakova  
*University of Wollongong, olga@uow.edu.au*

Wai Kong Yeoh  
*University of Sydney*

*See next page for additional authors*

Follow this and additional works at: <https://ro.uow.edu.au/engpapers>



Part of the [Engineering Commons](#)

<https://ro.uow.edu.au/engpapers/4162>

---

### Recommended Citation

Senatore, C.; Lezza, P.; Lortz, R.; Shcherbakova, Olga V.; Yeoh, Wai Kong; Dou, S. X.; and Flukiger, R.: Specific heat and magnetic relaxation analysis of MgB<sub>2</sub> bulk samples with and without additives 2007, 2941-2944.

<https://ro.uow.edu.au/engpapers/4162>

---

**Authors**

C. Senatore, P. Lezza, R. Lortz, Olga V. Shcherbakova, Wai Kong Yeoh, S. X. Dou, and R. Flukiger

# Specific Heat and Magnetic Relaxation Analysis of MgB<sub>2</sub> Bulk Samples With and Without Additives

C. Senatore, P. Lezza, R. Lortz, O. Shcherbakova, W. K. Yeoh, S. X. Dou, and R. Flükiger

**Abstract**—The effects of SiC and Carbon doping on the superconducting properties of MgB<sub>2</sub> polycrystalline samples have been analysed by means of specific heat and magnetic relaxation measurements. It is known that the addition of nanometric powders of SiC and C leads to the enhancement of  $B_{irr}$  and  $J_c$ . However, the underlying physical mechanism is not completely understood. Magnetic relaxation measurements did not show detectable effects of both the additions on the pinning properties of MgB<sub>2</sub>. It follows that doping acts mainly introducing disorder into the superconductor and thus raising  $B_{c2}$ . In the case of MgB<sub>1.9</sub>C<sub>0.1</sub>, specific heat measurements show that the C substitution on the B sites modifies the low temperature shoulder related to the second gap. This effect is not visible in the sample doped with SiC. From the distribution of  $T_c$  determined from the deconvolution of the calorimetric data, we argue that SiC leads to an inhomogeneous distribution of C.

**Index Terms**—Magnetic relaxation, MgB<sub>2</sub>, nanodoping, specific heat.

## I. INTRODUCTION

THE critical current density  $J_c$ , the upper critical field  $B_{c2}$  and in particular the irreversibility field  $B_{irr}$  are the central parameters in view of power applications of MgB<sub>2</sub>. Since the discovery of superconductivity in MgB<sub>2</sub>, extensive research on chemical substitutions was undertaken in order to improve its current carrying capability at increasing magnetic fields [1]. Among a large number of dopants, carbon substitution for boron appears to be the most promising one, though the reported carbon solubility in MgB<sub>2</sub> and its influence on  $T_c$  vary considerably depending on both the synthesis route and the starting materials [2]. Substantially improved  $J_c$  was observed in B<sub>4</sub>C doped MgB<sub>2</sub> bulk samples and Fe/MgB<sub>2</sub> wires at 4.2 K under high magnetic fields [3], [4]. Dou *et al.* [5], [6] reported the improvement of the critical current density in MgB<sub>2</sub> polycrystalline samples and Fe/MgB<sub>2</sub> wires by nanopowders of SiC and Carbon. In particular, the improvement of the current transport properties is easily achieved by nano SiC doping at a sintering temperature of 650°C [5]. On the other side, carbon

doping is effective at higher sintering temperatures, around 1000°C [6]. Nevertheless, the underlying physical mechanism remains still unclear. It is known that carbon doping is effective for introducing disorder into MgB<sub>2</sub>. This disorder shortens the coherence length of the superconductor (“dirty limit”) and is responsible for the interband scattering [7]; both the effects play an important role in raising the upper critical field. SiC is an effective carbon source acting as a dopant for MgB<sub>2</sub>. In addition the lower sintering temperature required to prepare SiC doped MgB<sub>2</sub> is thought to lead to a smaller grain size and thus to a higher grain boundary density. Since grain boundaries act as the main pinning mechanism in MgB<sub>2</sub> [8], the addition of SiC has been invoked as the responsible for a more effective pinning.

On the basis of these considerations, we report on magnetic relaxation and specific heat measurements of sintered polycrystalline samples of MgB<sub>2</sub>, binary and with C and SiC nanopowder additions. The time relaxation of the magnetization allowed us to probe the effect of the two additives on the pinning properties of MgB<sub>2</sub>. Moreover, a deconvolution of the specific heat data was used to determine the distribution of  $T_c$  in the samples in order to investigate possible inhomogeneities due to the local variation of the C content or to the morphology of the grains.

## II. SAMPLE PREPARATION AND DESCRIPTION

Three polycrystalline MgB<sub>2</sub> bulk samples have been studied in this work. The samples were prepared at the Institute for Superconductivity and Electronic Materials (ISEM) of the University of Wollongong. Powders of magnesium (99%) and amorphous boron (99%) were mixed for the fabrication of the binary MgB<sub>2</sub>. For processing the SiC doped MgB<sub>2</sub> sample, a mixture of Mg:2B with 10 wt.% SiC nanoparticles (size of 20-30 nm) was prepared. In both the cases the pellets were sintered at 800°C for 30 min. The third sample was doped with nanocarbon powders at the nominal composition of MgB<sub>1.9</sub>C<sub>0.1</sub> and sintered at 1000°C.

A first characterization of the samples was performed by AC susceptibility (Fig. 1). The temperatures corresponding to the onset and to the 10% of the superconducting transition are reported in Table I for the three samples. The MgB<sub>2</sub> and MgB<sub>1.9</sub>C<sub>0.1</sub> samples exhibit a sharp transition whereas  $\Delta T = 2$  K is found in the case of the sample with SiC addition.

The inductive critical current density  $J_c$  has been extracted from the magnetization loops using the Bean model formula

$$J_c = 30 \frac{\Delta M}{b} \frac{2}{3 - \frac{b}{a}} \quad (1)$$

Manuscript received August 28, 2006. This work was supported by the Swiss National Science Foundation through the National Centre of Competence in Research Materials with Novel Electronic Properties (MaNEP).

C. Senatore, R. Lortz, and R. Flükiger are with the Département de Physique de la Matière Condensée & MaNEP, Université de Genève, Geneva CH-1211, Switzerland (e-mail: carmine.senatore@physics.unige.ch; rolf.lortz@physics.unige.ch; rene.flukiger@physics.unige.ch).

P. Lezza is with the Groupe de Physique Appliquée, Université de Genève, Geneva CH-1211, Switzerland (e-mail: paola.lezza@physics.unige.ch).

O. Shcherbakova and S. X. Dou are with the Institute for Superconductivity and Electronic Materials, University of Wollongong, Wollongong NSW-2522, Australia (e-mail: os966@uow.edu.au; shi@uow.edu.au).

Digital Object Identifier 10.1109/TASC.2007.899556

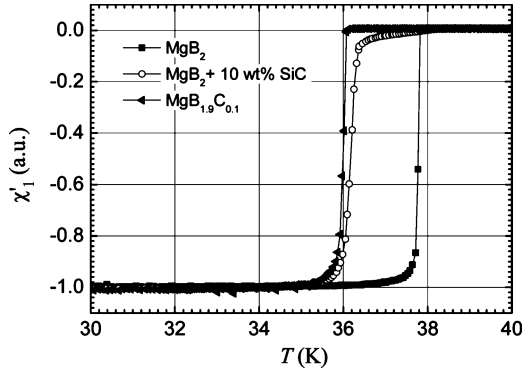


Fig. 1. Superconducting transition from AC susceptibility measurements for  $\text{MgB}_2$  (solid squares),  $\text{MgB}_2 + 10 \text{ wt}\% \text{ SiC}$  (open circles) and  $\text{MgB}_{1.9}\text{C}_{0.1}$  (solid triangles).

TABLE I  
NOMINAL CARBON COMPOSITION AND CRITICAL TEMPERATURES  
OF THE SAMPLES

Sample	Nominal Carbon (at. %)	$T_{\text{onset}} [\chi_1'']$ (K)	$T_{10\%} [\chi_1'']$ (K)
$\text{MgB}_2$	0	38.4	37.8
$\text{MgB}_2 + 10 \text{ wt}\% \text{ SiC}$	3.7	38.3	36.3
$\text{MgB}_{1.9}\text{C}_{0.1}$	3.3	36.3	36.0

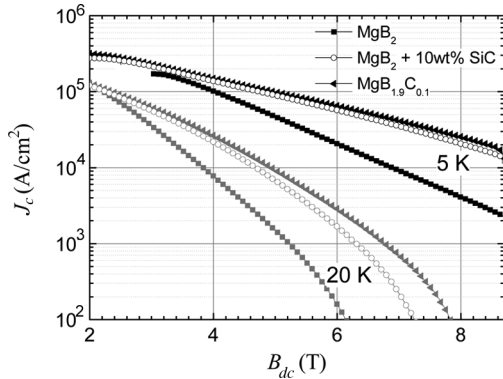


Fig. 2. Inductive critical current density  $J_c$  as a function of the magnetic field for  $\text{MgB}_2$  (solid squares),  $\text{MgB}_2 + 10 \text{ wt}\% \text{ SiC}$  (open circles) and  $\text{MgB}_{1.9}\text{C}_{0.1}$  (solid triangles) at  $T = 5 \text{ K}$  (black symbols) and  $20 \text{ K}$  (gray symbols).

where  $a$  and  $b$  are the dimensions in the basal plane ( $a > b$ ) and  $B$  perpendicular to this plane) and  $M$  is the irreversible magnetization.

Magnetic hysteresis loops have been measured using a vibrating sample magnetometer (VSM) equipped with a 9 T magnet. Fig. 2 shows the critical current density curves  $J_c(B)$  at 5 K and 20 K for the three samples. As is well known, the addition of SiC and C lead to higher critical current in magnetic field. By using the  $100 \text{ A/cm}^2$  criterion the irreversibility field  $B_{irr}$  has been determined at different temperatures. The resulting irreversibility lines are reported in Fig. 3. At  $T = 20 \text{ K}$   $B_{irr}$  is markedly higher for the samples with additives [3]–[6]. In the next section we will investigate the mechanisms related to the addition of nanoparticles being responsible for the improvement of the current transport properties.

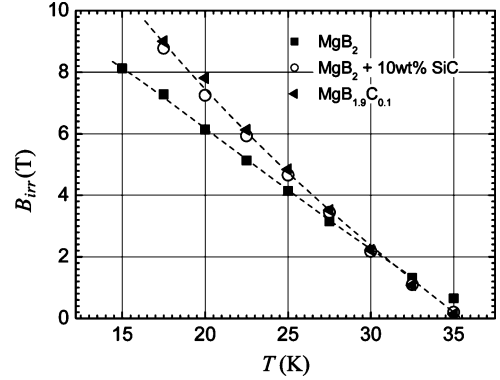


Fig. 3. Irreversibility lines determined from the inductive  $J_c(B)$  by using the  $100 \text{ A/cm}^2$  criterion for  $\text{MgB}_2$  (solid squares),  $\text{MgB}_2 + 10 \text{ wt}\% \text{ SiC}$  (open circles) and  $\text{MgB}_{1.9}\text{C}_{0.1}$  (solid triangles).

### III. EXPERIMENTAL RESULTS AND DISCUSSION

#### A. Magnetic Relaxation Measurements

The magnetic relaxation, arising from thermally activated flux creep, has been intensively studied in conventional and high temperature superconductors [9]. The magnetization decreases logarithmically in time. This logarithmic dependence is predicted in the framework of the Anderson-Kim model [10]. In fact, by considering the thermally activated motion of flux bundles in the presence of correlated defects, these authors obtained from the magnetic diffusion equation the following time dependence for the current density:

$$J = J_{c0} \left[ 1 - \frac{k_B T}{U_0} \ln \left( \frac{t}{t_0} \right) \right], \quad (2)$$

where  $U_0$  is the volume pinning energy for  $T = 0$  and  $B = 0$ ,  $t_0$  is a characteristic time scale. Since the magnetization  $M$  is proportional to  $J$  when the sample is fully penetrated by the field,  $M$  relaxes with the same logarithmic flux creep correction as the current density, given by (2). Moreover, the volume pinning energy is found to be inversely proportional to the normalized relaxation rate:

$$S = \frac{1}{M_0} \frac{dM}{d \ln t} = -\frac{k_B T}{U_0}, \quad (3)$$

where  $M_0$  is the magnetization corresponding to the unrelaxed value.

In our magnetic relaxation measurements magnetization was measured as a function of time for 6000 s, keeping the external field constant. Measurements have been performed at different dc fields from 0 to 8 T in the temperature range 5–20 K.

The standard logarithmic relaxation law  $M \propto \ln(t)$  is recovered for the three samples for  $t > 5 \text{ s}$ , as shown in Fig. 4 at  $T = 10 \text{ K}$  and  $B = 3 \text{ T}$ . Bearing in mind the simple relation between relaxation rates and pinning energy in (3), we compare in Fig. 5 the relaxation rates of  $\text{MgB}_2$ ,  $\text{MgB}_2 + 10 \text{ wt}\% \text{ SiC}$  and  $\text{MgB}_{1.9}\text{C}_{0.1}$ , as a function of the magnetic field at  $T = 5, 10$  and  $20 \text{ K}$ . Relaxation rates are defined as the decay of the magnetization (in %) over a decade of the time-log scale.

It is clear that the experimental points corresponding to the three different samples lie on the same line at each temperature. This means that additives do not lead to a strong improvement of

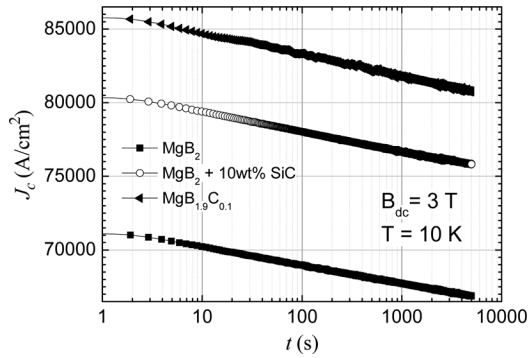


Fig. 4. Magnetic relaxation measurements at  $T = 10$  K and  $B_{dc} = 3$  T for MgB<sub>2</sub> (solid squares), MgB<sub>2</sub> + 10 wt.% SiC (open circles) and MgB<sub>1.9</sub>C<sub>0.1</sub> (solid triangles). The logarithmic behavior is recovered for  $t > 5$  s.

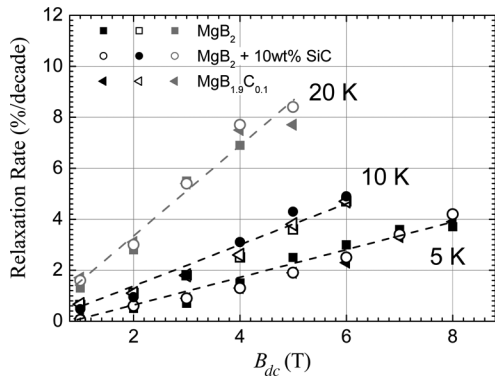


Fig. 5. Comparison of the relaxation rates of MgB<sub>2</sub> (squares), MgB<sub>2</sub> + 10 wt.% SiC (circles) and MgB<sub>1.9</sub>C<sub>0.1</sub> (triangles) at  $T = 5$  K, 10 K and 20 K.

pinning. In particular the precipitates of impurity phases in the case of the SiC additions do not act as additional pinning centers. This could be ascribed to the large size of these precipitates compared to the dimensions of the vortex bundles involved in the flux creep processes. The increased irreversibility fields for the samples doped with SiC and C are thus correlated to the enhancement of the upper critical field  $B_{c2}$ . Therefore, the effect of the additives is the introduction of disorder that drives the system MgB<sub>2</sub> in the dirty limit. In the following we will analyse the results of the specific heat measurements in order to verify if SiC and C introduce the same kind of disorder in MgB<sub>2</sub>.

### B. Specific Heat Measurements

The temperature dependence of the specific heat was measured from 2 to 45 K for the three MgB<sub>2</sub> samples, at zero field and at 14 T. Measurements were performed using a relaxation calorimeter [11]. A Cernox chip was employed as sample holder and thermometer/heater. The mass of the samples was 32.901 mg (MgB<sub>2</sub>), 19.083 mg (MgB<sub>2</sub> + 10 wt.% SiC) and 10.543 mg (MgB<sub>1.9</sub>C<sub>0.1</sub>).

The specific heat of the binary MgB<sub>2</sub> is shown in Fig. 6. At zero field the onset of the superconducting transition is at  $T = 38.4$  K, whereas superconductivity is suppressed at 14 T.

The superconducting transition of the three samples has been isolated from the phononic background by subtracting the specific heat curves measured at high field from those measured in zero field. The resulting superconducting contributions are illustrated in Fig. 7. The jump at  $T_c$  is well pronounced for the binary

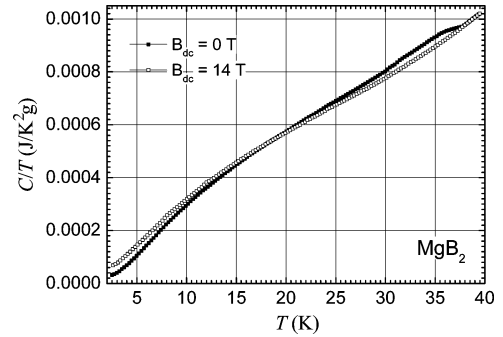


Fig. 6. Specific heat versus  $T$  for the MgB<sub>2</sub> sample, at zero field (solid squares) 14 T (open squares).

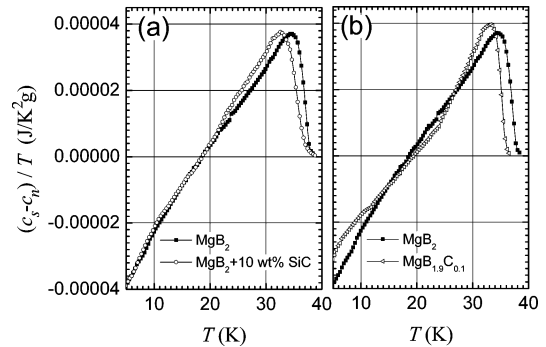


Fig. 7. Superconducting contribution to the specific heat: (a) MgB<sub>2</sub> versus MgB<sub>2</sub> + 10 wt.% SiC; (b) MgB<sub>2</sub> versus MgB<sub>1.9</sub>C<sub>0.1</sub>.

and the Carbon doped samples but gets broader with the SiC addition. The specific heat in the superconducting state exhibits for all samples an excess at low temperature when compared to the conventional single gap BCS behavior. This is a peculiar feature of the two gap nature of the superconductivity in MgB<sub>2</sub>. Within the two gap model, two electronic bands, characterized by two different superconducting gaps, contribute to the specific heat proportionally to their partial density of states [12]. In the case of substitution of C on the B sites, the density of the states of the band corresponding to the smaller gap is changed. This is the case for the MgB<sub>1.9</sub>C<sub>0.1</sub>, the low temperature shoulder related to the second gap being markedly changed with respect to the undoped sample. On the contrary the calorimetric transition of the MgB<sub>2</sub> + 10 wt.% SiC does not show any change in the low temperature region, the effect of the C substitution on the second gap shoulder being hidden by the distribution of  $T_c$  in the sample. At this point the superconducting contributions to the specific heat have been analysed by means of a particular deconvolution method in order to determine the distribution of  $T_c$  [13], [14]. The distributions of the critical temperature are reported in Fig. 8 for the three samples. The onset  $T_c$  and the half height width of the distributions are reported in Table II. The half height  $\Delta T$  was found to increase with the SiC added sample, while the width of the distributions for the MgB<sub>2</sub> and MgB<sub>1.9</sub>C<sub>0.1</sub> results to be comparable.

From the different behavior encountered in the specific heat of the MgB<sub>1.9</sub>C<sub>0.1</sub> and MgB<sub>2</sub> + 10 wt.% SiC samples we can argue that the SiC addition leads to an inhomogeneous distribution of C. This inhomogeneity masks the effect of the substitution of C for B on the second gap shoulder. In both the doped samples, the C substituted on the B sites introduces scattering

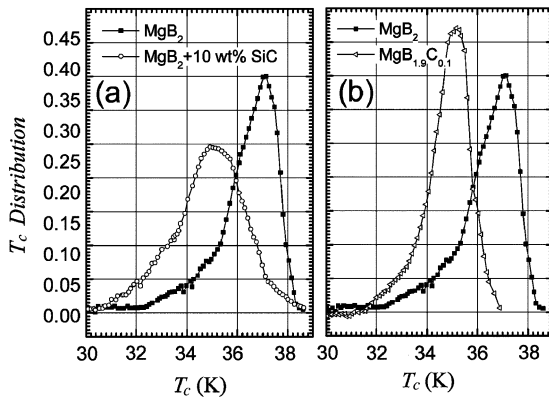


Fig. 8. Distribution of  $T_c$  obtained by the deconvolution of the specific heat data: (a)  $\text{MgB}_2$  versus  $\text{MgB}_2 + 10 \text{ wt. \% SiC}$ ; (b)  $\text{MgB}_2$  versus  $\text{MgB}_{1.9}\text{C}_{0.1}$ .

TABLE II  
DISTRIBUTION OF  $T_c$ : ONSET TEMPERATURE AND HALF HEIGHT WIDTH

Sample	Onset $T_c$ (K)	half height $\Delta T_c$ (K)
$\text{MgB}_2$	38.4	1.9
$\text{MgB}_2 + 10 \text{ wt. \% SiC}$	38.3	2.9
$\text{MgB}_{1.9}\text{C}_{0.1}$	36.6	1.6

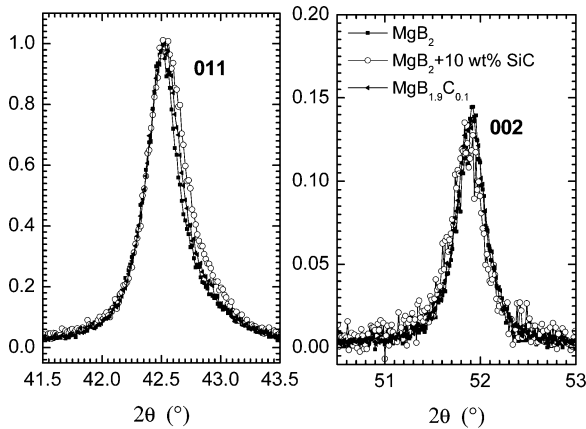


Fig. 9. Selected regions of the X-ray diffraction pattern for the three  $\text{MgB}_2$  samples. As a consequence of the additions, a shift is clearly identified in the 101 peak, but not in the 002 peak.

centers that reduce the electron mean free path and thus raises  $B_{c2}$ .

In Fig. 9 we report the X-ray diffraction data for the three samples in correspondence of selected regions of the pattern. The same value of the  $a$  lattice parameter is found for the two doped samples (see Table III). This indicates that the average substitutional level of the C on the B sites is similar. However, the (101) peak of the  $\text{MgB}_2 + 10 \text{ wt. \% SiC}$  exhibits a larger full width at half maximum respect to the other two samples. This

TABLE III  
LATTICE PARAMETERS

Sample	$a$ (Å)	$c$ (Å)
$\text{MgB}_2$	3.0853(2)	3.5259(3)
$\text{MgB}_2 + 10 \text{ wt. \% SiC}$	3.0777(3)	3.5268(3)
$\text{MgB}_{1.9}\text{C}_{0.1}$	3.0776(2)	3.5259(2)

is a consequence of the inhomogeneous Carbon distribution, as already deduced from the specific heat analysis.

#### IV. SUMMARY

In the present study, we have investigated the effects of SiC and Carbon doping on the superconducting properties of  $\text{MgB}_2$  polycrystalline samples. From magnetic relaxation measurements, no sizeable effects were detected on the pinning properties of  $\text{MgB}_2$  which could be attributed to the presence of additives. The doping acts mainly by introducing disorder into the superconductor, thus raising  $B_{c2}$ . This happens by the C substitution on the B sites. As shown by specific heat measurements, in the case of SiC the distribution of  $T_c$  is broader as a consequence of an inhomogeneous distribution of C in the sample.

#### ACKNOWLEDGMENT

The authors would like to thank Mr. Michel Moret for the technical support in the design of the specific heat probe.

#### REFERENCES

- [1] R. J. Cava, H. W. Zandbergen, and K. Inumara, *Physica C*, vol. 385, p. 8, 2003.
- [2] A. Bharathi, S. Jemima Balaselvi, S. Kalavathi, G. L. N. Reddy, V. Sankara Sastry, Y. Hariharan, and T. S. Radhakrishnan, *Physica C*, vol. 370, p. 211, 2002.
- [3] A. Yamamoto, J. Shimoyama, S. Ueda, I. Iwayama, S. Horii, and K. Kishio, *Supercond. Sci. Technol.*, vol. 18, p. 1323, 2005.
- [4] P. Lezza, C. Senatore, R. Gladyshevskii, and R. Flükiger, *Supercond. Sci. Technol.*, vol. 19, p. 1030, 2006.
- [5] S. X. Dou, A. V. Pan, S. H. Zhou, M. Ionescu, X. L. Wang, J. Horvat, H. K. Liu, and P. R. Munroe, *J. Appl. Phys.*, vol. 94, p. 1850, 2003.
- [6] S. Soltanian, J. Horvat, X. L. Wang, P. R. Munroe, and S. X. Dou, *Physica C*, vol. 390, p. 185, 2003.
- [7] A. Gurevich, *Phys. Rev. B*, vol. 67, p. 184515, 2003.
- [8] C. Senatore, P. Lezza, and R. Flükiger, *Adv. Cry. Eng.*, vol. 53, p. 654, 2006.
- [9] Y. Yeshurun, A. P. Malozemoff, and A. Shaulov, *Rev. Mod. Phys.*, vol. 68, p. 911, 1996.
- [10] P. W. Anderson and Y. B. Kim, *Rev. Mod. Phys.*, vol. 36, p. 39, 1964.
- [11] D. Sanchez, A. Junod, J.-Y. Genoud, T. Graf, and J. Muller, *Physica C*, vol. 200, p. 1, 1992.
- [12] F. Bouquet, R. A. Fisher, N. E. Phillips, D. G. Hinks, and J. D. Jorgensen, *Phys. Rev. Lett.*, vol. 87, p. 047001, 2001.
- [13] A. Junod, T. Jarlborg, and J. Muller, *Phys. Rev. B*, vol. 27, p. 1569, 1983.
- [14] Y. Wang, C. Senatore, V. Abächerli, D. Uglietti, and R. Flükiger, *Supercond. Sci. Technol.*, vol. 19, p. 263, 2006.